Organic & Biomolecular Chemistry

Cite this: *Org. Biomol. Chem.*, 2011, **9**, 6788

www.rsc.org/obc

PAPER

Synthesis of mono- and di-[12]aneN$_3$ ligands and study on the catalytic cleavage of RNA model 2-hydroxypropyl-*p*-nitrophenyl phosphate with their metal complexes†

Zhi-Fo Guo, Hao Yan, Zhi-Fen Li and Zhong-Lin Lu*

Received 11th June 2011, Accepted 22nd July 2011
DOI: 10.1039/c1ob05942d

A series of mono- and di-[12]aneN$_3$ ligands **1–6**, which contain different substituents on the coordinating backbone, different linkers between two [12]aneN$_3$ units and different *N*-methylation on the [12]aneN$_3$ units, have been synthesized and fully characterized. The catalytic activities of their metal complexes on the cleavage of RNA model phosphate 2-hydroxypropyl-*p*-nitrophenyl phosphate (HPNPP) varied with the structures of the ligands and metal ions. Click reactions afforded an efficient method to prepare a series of [12]aneN$_3$ ligands, however, the incorporation of triazole moieties reduced the catalytic activities due to their coordination with metal ions and the strong inhibition from the triflate counter ion. Dinuclear zinc(II) complexes containing an *m*-xylyl bridge showed higher catalytic activities with synergistic effects up to 700-fold. Copper(II) complexes with the ligands without triazole moieties proved to be highly reactive and showed strong cooperativity between the two copper(II) ions. In terms of k_2, dinuclear complexes Zn_2-**3b**, Zn_2-**3d**, Zn_2-**4b**, and Cu_2-**4b** afforded activities of 7.9×10^5, 3.9×10^4, 9.0×10^4, and 8.1×10^4-fold higher than that of methoxide. The *ortho* arrangement of the two [12]aneN$_3$ units and the presence of 5- or 2-positioned substituents in the benzene ring as well as *N*-methylation of [12]aneN$_3$ units greatly reduced the catalytic activities due to the steric effects. These results clearly indicate that the structures of the linker between two [12]aneN$_3$ units play very important role in their catalytic synergistic effects.

Introduction

Intensive work has been focused on the development of small synthetic metallonucleases for the cleavage of the phosphodiester bond in RNA, DNA, and their model compounds.[1–6] These studies are beneficial for shedding light on understanding the chemistry of the corresponding hydrolytic enzymes, providing artificial restriction enzymes for molecular biology which would be highly valuable in the manipulation of DNA, and developing antibiotic and chemotherapeutic drugs. It has been shown that many of the nucleases have active sites comprising two or more metal ions. For example, alkaline phosphatase possesses dinuclear Zn^{2+} and Mg^{2+} centers, purple acid phosphatase employs a center containing one Fe^{3+} and one Fe^{2+} or Zn^{2+} ions, while P1 nuclease contains a trinuclear Zn^{2+} active site and ribonuclease H from HIV reverse transcriptase contains a two-metal ion active site.[7–9] For these reasons, many studies have been devoted to the design and synthesis of dinuclear or polynuclear metal complexes.[10–12]

Among the dinuclear systems developed by the spacer strategy, ligands containing 1,4,7-triazacyclononane ([9]aneN$_3$)[1,13] 1,5,9-triazacyclododecane ([12]aneN$_3$),[14–16] 1,4,7,10-tetraazacyclododecane ([12]aneN$_4$)[17,18] units are very promising in the development of artificial nucleases. Recently, Brown's group has investigated a system of dinuclear metal complexes of 1,3-*bis*-N$_1$-(1,5,9-triazacyclododecyl)propane (abbreviated as PP-Di-[12]aneN$_3$, see Scheme 1) in methanol and ethanol and found that they can accelerate the cleavage of model phosphate diesters by a remarkable factor of up to $10^{12–14}$-fold, when compared to the background reactions.[2,19] The excellent catalytic performance of the system has been attributed to the medium effect with lower dielectric constants and the synergistic effect between metal ions.

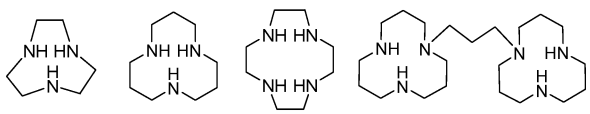

Scheme 1 Structures of [9]aneN$_3$, [12]aneN$_3$, [12]aneN$_4$, and PP-Di-[12]aneN$_3$.

College of Chemistry, Beijing Normal University, Xinjiekouwai Street 19, Beijing, 100875, China. E-mail: luzl@bnu.edu.cn; Fax: +86-10-58801804; Tel: +86-10-58801804

† Electronic supplementary information (ESI) available: Tables of kinetic data and method for triflate ion inhibition, plots of kinetics data as a function of metal complex concentrations and triflate; NMR and mass spectroscopic data for ligands **1–6** and the intermediates. See DOI: 10.1039/c1ob05942d

Previous work demonstrates that the distances between the two coordinating moieties, the structures of the linkers, and the secondary coordination spheres of the ligands all play important roles in achieving good catalytic activity for the dinuclear metal complexes. With the above considerations, we report here on the synthesis and characterization of a series of mono- and di-[12]aneN$_3$ ligands containing different substituents on the coordinating backbone, different linkers between two [12]aneN$_3$ units as well as different steric coordinating spheres (see Scheme 2). The catalytic activities of their zinc(II) and copper(II) complexes on the cleavage of RNA model phosphate 2-hydroxypropyl-4-nitrophenyl phosphate (HPNPP) have been investigated and are reported here.

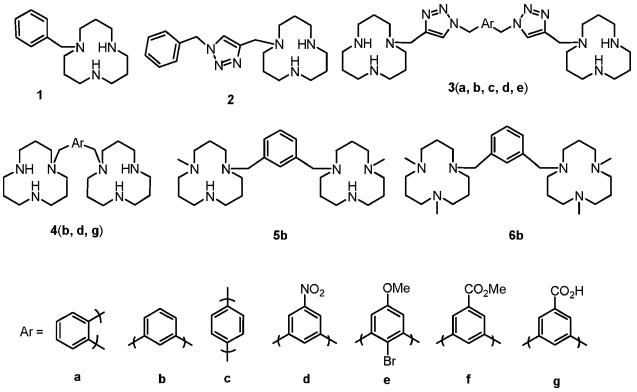

Scheme 2 Structures of the mono- and di-[12]aneN$_3$ ligands.

Results and discussion

Syntheses and characterization of ligands 1–6

We synthesized new [12]aneN$_3$ ligands for our artificial nucleases study using two different strategies (Schemes 3 and 4).

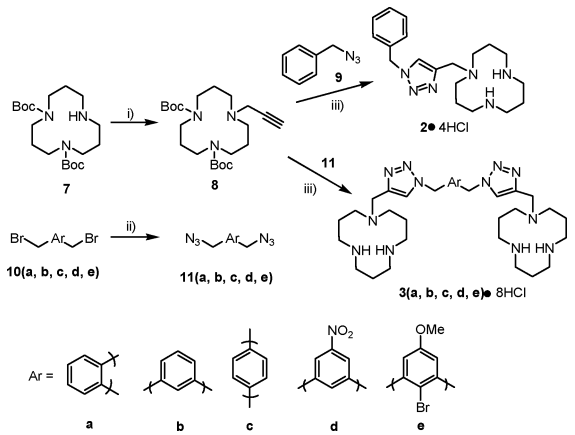

Scheme 3 Syntheses of **2** and **3**: i) propargyl bromide, THF, NEt$_3$, reflux 72h; ii) NaN$_3$, THF/H$_2$O; iii) a) THF/H$_2$O, CuSO$_4$, Vc; b) CH$_3$COCl, CH$_3$OH.

Ligands **2** and **3** were prepared by using highly efficient Cu(I)-catalyzed alkyne-azide cycloaddition reactions.[20] The mono- and bis-azido compounds were prepared from their corresponding bromides, which were in turn prepared from the bromination of substituted xylenes following the modified literature

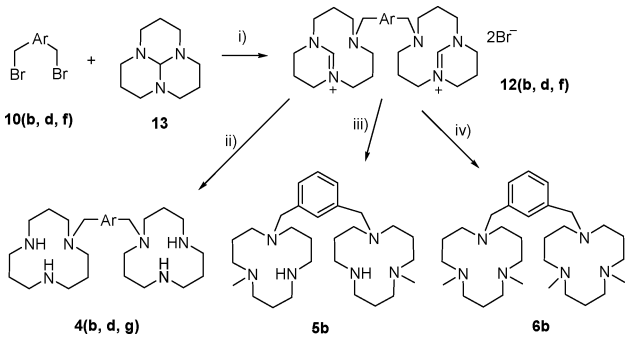

Scheme 4 Syntheses of ligand **4–6**: i) **13**, CHCl$_3$, reflux 2 h; ii) 3 M HCl, 12 h; iii) NaBH$_4$, EtOH, overnight; iv) HCHO, HCOOH, reflux overnight.

method.[21] The terminal alkyne, di-*tert*-butyl-1-propargyl-1,5,9-triazacyclododecane-5,9-tricarboxylate **8**, an important building block for the construction of multi-[12]aneN$_3$ compounds, was prepared from the reaction between di-*tert*-butyl-1,5,9-triazacyclododecane-5,9-tricarboxylate **7** and propargyl bromide in the presence of triethylamine. The click reactions between alkyne **8** and azides afforded the Boc-protected products in high yields. The removal of the Boc protecting groups was accomplished in anhydrous methanol in the presence of acetyl chloride at room temperature for 1 h. The resultant hydrochloride salts of ligands **2** and **3**, which are stable at room temperature for long period of time and are easily handled for their further use, were fully characterized. In the ^{1}H-NMR spectra, the protons from triazole moieties generally appear at 8.10–8.19 ppm in a singlet, the protons from the CH$_2$ moieties at the 1-and 4- positions of the triazole units appear at 4.18–4.37 (singlet) and 5.62–5.76 (singlet, CH$_2$Ar) ppm, respectively. The protons from the aryl moieties appear in the range of 6.98–8.07 ppm and their splitting is consistent with their substitution mode. The protons from the methylene groups of the [12]aneN$_3$ units generally appear around 2.20, 3.10 and 3.30 ppm as multiplets, and are consistent with those reported in the literature.[16,22,23]

The synthesis of ligands **4–6** began with the alkylation reactions between the [12]aneN$_3$ precursor **13** and either 1,3-bis(bromomethyl)benzene **10b** or 5-substituted-1,3-bis- (bromomethyl)benzenes **10d/10f**. Depending on the following work-up procedure, the intermediates **12b/d/f** were converted to non-methyl, dimethyl, and tetramethyl substituted compounds **4b/d/f**, **5b**, and **6b**. Although compounds **4b** and **6b** have been reported previously,[24,25] no detailed characterization data were provided. In the ^{1}H-NMR spectra, the protons from the CH$_2$ group between the aryl and [12]aneN$_3$ units are located at 3.38–3.57 ppm. The methyl groups on the [12]aneN$_3$ unit appear at 2.08–2.20 ppm, and the integration of the protons are consistent with the structure. The chemical shifts of the protons on the aryl and [12]aneN$_3$ groups are consistent with those in the literature.[16,22,23,26]

Spectroscopic study of the coordination behavior of ligand 2

Click reactions afforded the efficient preparation of various [12]aneN$_3$ ligands containing the triazole moieties in this work. Since copper(II) complexes of the *N*-ligands are highly colored, the changes in the immediate coordination environment surrounding the metal ion can be inferred from the electronic spectra. To get information about the coordination of the triazole moiety

to copper ion, the visible spectra of Cu-**2** together with Cu-**1** and Cu-[12]aneN$_3$ were recorded in methanol and are shown in Fig. 1. The maximum peaks of the absorption appear at 681, 669, and 659 nm for complexes Cu-[12]aneN$_3$, Cu-**1**, and Cu-**2**, respectively. The blue shift of the maximum absorption and the appearance of a shoulder around near 780 nm clearly indicated that the presence of the triazole moiety in ligand **2** resulted in the change of coordination geometry of the copper(II) ion.[27,28]

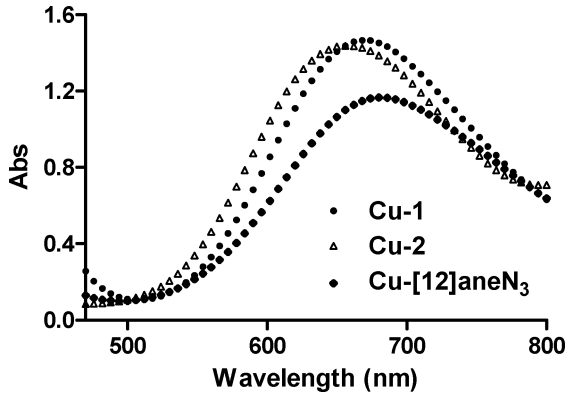

Fig. 1 UV spectra of Cu-[12]aneN$_3$, Cu-**1**, and Cu-**2** at 8.0 mM in methanol.

Catalytic cleavage of HPNPP

We have evaluated the catalytic activities of the metal complexes of ligands **1–6** on the cleavage of 2-hydroxypropyl-*p*-nitrophenyl phosphate (HPNPP) (Scheme 5), which is often used as model compound of RNA.[1,5,19] To avoid the effect of triflate counter ions, the kinetic data for all zinc(II) and some copper(II) complexes were corrected for their respective triflate inhibition constants (see supporting information)

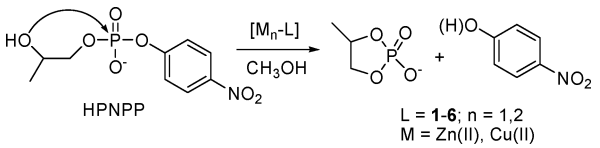

Scheme 5 Cleavage of HPNPP catalyzed by metal complexes of **1–6**.

i) Cleavage of HPNPP with mononuclear metal complexes. Fig. 2 shows the plots of the corrected observed pseudo-first order rate constants for the cleavage of HPNPP as a function of [M:L] (M = Zn(II), Cu(II), L = **1**, **2**) in the presence of 0.5 eq. of CH_3O^- to set the ^s_spH of the solution to self-buffered conditions.

For ligand **1**, the plots of Cu-**1** and Zn-**1** show a slight upward curvature, indicating a bimolecular process which is similar to that of Zn-[12]aneN$_3$ in the literature.[29] By fitting the plots in the eqn (1), it affords k_2^{obs} and k_3^{obs} for Cu-**1** and Zn-**1**, respectively.

$$k^{obs} = k_2^{obs}[\text{M-}\mathbf{1}] + k_3^{obs}[\text{M-}\mathbf{1}]^2 \quad (1)$$

For ligand **2**, the plots of both Zn-**2** and Cu-**2** are bowed, which is not due to substrate-complex saturation binding process but rather a monomer-dimer equilibrium behaviour, which requires a square-root dependence.[30] The data can be fit *via* a standard NLLSQ treatment to eqn (2), which affords the dimer dissociation

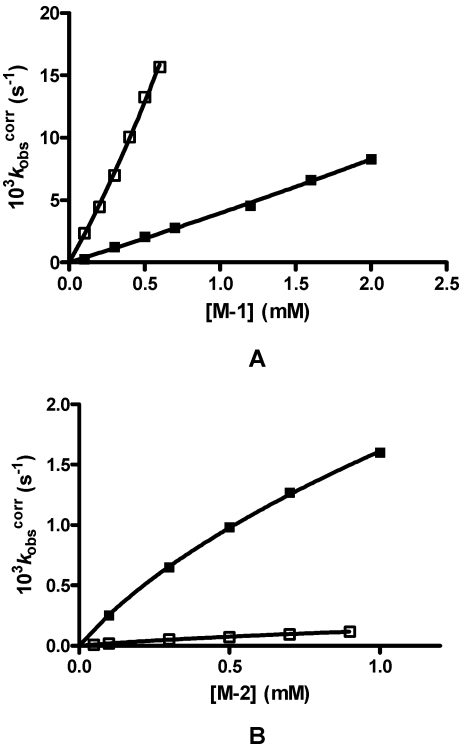

Fig. 2 Plots of k_{obs} *vs.* [M-**L**] (M = Zn(II) ■, Cu(II) □) for the cleavage of HPNPP (4.0×10^{-5} M) at [$^-$OCH$_3$]/[M(II)] = 0.5 and 25.0 ± 0.1 °C. (A) **L** = **1**, ^s_spH = 10.0 ± 0.1 for Zn-**1** and ^s_spH = 8.9 ± 0.1 for Cu-**1**. (B) **L** = **2**, ^s_spH = 10.0 ± 0.1 for Zn-**2** and ^s_spH = 8.8 ± 0.1 for Cu-**2**.

Table 1 Kinetic data for the cleavage of HPNPP mediated by the mononuclear complexes of ligands **1** and **2** at 25.0 ± 0.1 °C

Cat	10^3K_{dis} (M)	k_2 (M^{-1} s^{-1})	10^3k_3 (M^{-2} s^{-1})
$^-$OMe	—	2.56×10^{-3}[a]	—
Zn-[12]aneN$_3$	—	18.9[a]	1.8 ± 0.4[a]
Cu-[12]aneN$_3$	—	23.17[b]	—
Zn-**1**	—	3.8 ± 0.2	0.18 ± 0.11
Cu-**1**	—	21.5 ± 1.2	8.5 ± 2.5
Zn-**2**	1.4 ± 0.2	2.9 ± 0.2	—
Cu-**2**	1.7 ± 0.6	0.21 ± 0.02	—

[a] See reference 31. [b] The measured k_2 see supporting information.

constant (K_{dis}) and conditional second rate constant (k_m) for the reactive mononuclear complex.

$$k_{obs} = \{k_m K_{dis}(\sqrt{1 + 8[M^{2+}]_t/K_{dis}} - 1)\}/4 \quad (2)$$

All of the kinetic data are listed in Table 1. It can be seen that the second-order rate constant of Cu-**1** (21.5 M^{-1} s^{-1}) is the highest among the mononuclear complexes in this study, which is 8.5 × 10^3-fold higher than that of methoxide (2.56×10^{-3} M^{-1} s^{-1}).[31]

For the mononuclear zinc(II) complexes, incorporating benzyl and benzyl-triazole moieties reduced the activity. Compared to benzyl substituent in Zn-**1**, the presence of the triazole group in Zn-**2** further reduced the activity but not significantly. For the mononuclear copper(II) complexes, apparently the presence of the benzyl group has almost no effect on the catalytic activity when compared to that of the Cu-[12]aneN$_3$ complex. However, the

Table 2 Kinetic constants (maximum catalytic pH rate constant (k^{max}), dissociation constants (K_M) and second order rate constants (k_2 or k^{max}/K_M) for the cleavage of HPNPP mediated by different dinuclear catalysts at 25.0 ± 0.1 °C

Catalysts	${}^{s}_{s}$pH	K_i (OTf)(mM)	$10^3 k^{max}$ (s^{-1})[a]	$10^3 K_M$ (M)	k_2 (M^{-1} s^{-1})	Synergistic effect
Zn_2-**3a**	9.8 ± 0.1	2.4 ± 0.3	20.3 ± 2.6	0.31 ± 0.07	65 ± 15	22[b]
Zn_2-**3b**	10.1 ± 0.1	0.20 ± 0.21	—	—	2030 ± 120	700[b]
Zn_2-**3c**	9.9 ± 0.1	1.4 ± 0.3	—	—	105 ± 3.8	36[b]
Zn_2-**3d**	9.2 ± 0.1	0.59 ± 0.08	—	—	99.6 ± 2.7	34[b]
Zn_2-**3e**	10.2 ± 0.1	3.98 ± 0.13	7.9 ± 0.4	0.29 ± 0.04	27.2 ± 3.7	9[b]
Zn_2-**4b**	9.6 ± 0.1	8.7 ± 1.1	—	—	231 ± 12	61[c]
Zn_2-**4d**	9.8 ± 0.1	10.3 ± 0.7	16.1 ± 0.6	0.70 ± 0.04	23.0 ± 0.8	6[c]
Zn_2-**4g**	10.1 ± 0.1	—	7.9 ± 1.3	0.23 ± 0.09	34 ± 13	9[c]
Zn_2-**5b**	9.9± 0.1	—	19.5 ± 1.5	0.99 ± 0.15	19.7 ± 1.5	5[c]
Zn_2-**6b**	9.8 ± 0.1	—	4.2 ± 0.2	0.39 ± 0.07	10.8 ± 1.9	3[c]
Cu_2-**3d**	7.9 ± 0.2	9.7± 0.8	1.27 ± 0.05	0.13 ± 0.02	9.8 ± 1.5	—
Cu_2-**4b**	9.2 ± 0.1	—	—	—	209 ± 2	10[d]
Cu_2-**4d**	6.9 ± 0.2	14.1± 0.8	12.2 ± 2.5	1.01± 0.26	12.1± 2.5	—

[a] k^{max} and K_M determined by fits of the Michaelis–Menten equation. [b] Compared to that of Zn-**2**. [c] Compared to that of Zn-**1**. [d] Compared to that of Cu-**1**.

incorporation of the triazole moiety in Cu-**2** dramatically reduced the catalytic activity by 100-fold.

The different catalytic performances of M-**1** and M-**2** can be attributed to their different coordination behavior in the bimolecular process. It is known that [12]aneN$_3$ coordinates to metal ions through its three nitrogen donors in a facial mode, the coordination geometries are four-coordinate tetrahedral for zinc(II) ion and five-coordinate square-pyramidal for copper(II) ion.[32] Generally, copper(II) ion can strongly coordinate to nitrogen donors. Thus the triazole moiety in **2** can coordinate to copper(II) ion and leave one less coordinate site available for the activation of a substrate or a nucleophile. This has been supported by the UV-Visible spectroscopic study (Fig. 1). The coordination of triazole moieties to copper(II) ions has also been reported.[33]

ii) Cleavage of HPNPP with dinuclear metal complexes. The catalytic cleavage of HPNPP in the presence of zinc(II) and copper(II) complexes of ligand **3(a–e)**, **4(b**, **d**, **g)**, **5b** and **6b** were carried out under self-buffered conditions as described in the Experimental Section and Supporting Information. In the preliminary work, the reaction conditions were optimized by varying equivalents of base ($NaOCH_3$), metal ion, and by mixing time. It was found that the catalysts formed by the literature procedure[29] are the most active, *i.e.* the catalysts were obtained *in situ* through sequential addition of stock solutions of sodium methoxide, macrocyclic polyamine ligand, and $Zn(OTf)_2$ (or $Cu(OTf)_2$) to anhydrous methanol such that $[CH_3O^-]$: [di-[12]aneN$_3$] : [M(II)] = 1 : 1 : 2.[29]

a) The cleavage of HPNPP with dinuclear metal complexes containing triazole moieties. Ligands **3a–3c** contain two triazole-attached [12]aneN$_3$ units but with different spatial arrangements. We observed a strong inhibition from triflate counter ions on catalytic rate constants for the dinuclear zinc(II) complexes (see K_i data in Table 2). After correcting for the triflate inhibition, the plots of k_{obs} *versus* [catalyst] are shown in Fig. 3, which indicates that the arrangement of the two [12]aneN$_3$ units plays an important role in the catalysis.

It is apparent that *ortho* substituted Zn_2-**3a** provided much poorer catalytic activity, the plot of k_{obs}^{corr} *versus* [Zn_2-**3a**] shows a saturation curve. Fitting the data with the Michaelis–Menten eqn

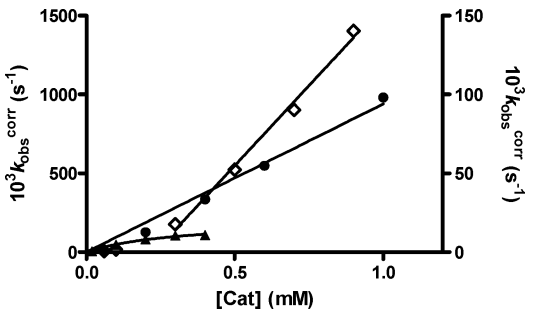

Fig. 3 Plots of k_{obs} *vs.* Zn_2-**3** (**3a** ▲, **3b** ◇, **3c** ●) for the cleavage of HPNPP (4.0×10^{-5} M) at [$^-OCH_3$]/[Zn(II)] = 0.5, ${}^{s}_{s}$pH = 9.8 ± 0.1 for Zn_2-**3a** (right axis), ${}^{s}_{s}$pH = 10.1 ± 0.1 for Zn_2-**3b** and ${}^{s}_{s}$pH = 9.9 ± 0.1 for Zn_2-**3c** at 25.0 ± 0.1 °C.

(3) afforded k^{max} and K_M to be (20.3 ± 2.6) $\times 10^{-3}$ s^{-1} and 0.31 ± 0.07 mM.

$$k_{obs} = k^{max}[Sub]/(K_M + [Sub]) \quad (3)$$

For the *meta*-substituted di-[12]aneN$_3$ system Zn_2-**3b**, it was found that k_{obs}^{corr} increased sharply beyond 0.2 mM of Zn_2-**3b** and showed linearity at higher concentration ranges of the measurement. It was assumed that the dinuclear complex for Zn_2-**3b** was not fully formed at lower concentrations. The gradient of the linear part of the plot gave a second rate constant of (2.03 ± 0.12) × 10^3 M^{-1} s^{-1}. The plot of k_{obs}^{corr} *versus* [Zn_2-**3c**] is almost linear, and the second order rate constant for the catalytic processes (k_2), evaluated from the gradients of the linear plot, is 105.1 ± 3.8 M^{-1} s^{-1}.

The plots of k_{obs} *versus* [catalyst] for the dinuclear zinc(II) complexes of **3d** and **3e** (Figure 4S) showed linear dependence and saturation dependence, respectively. The analyzed kinetic data are listed in Table 2. It is obvious that incorporating a substituent at the 5- and 2-position of the *meta*-substituted di-[12]aneN$_3$ system reduced the catalytic activity.

When it came to the copper complexes of the above di-[12]aneN$_3$ ligands, the catalytic properties dramatically decreased. For example, the catalytic activity of Cu_2-**3d** was much lower and showed a saturation kinetics with k^{max} of (1.27± 0.05) × 10^{-3} s^{-1} (see Figure 9S). Even after the correction of triflate inhibition

which is obviously not strong when compared with those of the corresponding zinc(II) complex, the calculated k_2 is lower than that of Cu-**1**.

All of the kinetic data are listed in Table 2. It can be seen that Zn_2-**3b** in this series showed the highest catalytic activity with the second-order rate constant of 2.03×10^3 M^{-1} s^{-1} after correcting for triflate inhibition. Compared with the activity of the mononuclear complex Zn-**2**, Zn_2-**3b** showed synergistic effects up to 700-fold between the two metal ions.

b) The cleavage of HPNPP with dinuclear complexes of 4–6. Further, we monitored the catalytic activity of the dinuclear metal complexes lacking the triazole moieties, *i.e.* di-[12]aneN$_3$ ligands **4–6**, which contain two [12]aneN$_3$ units linked directly by *meta*-xylyl backbones but with different steric effects.

The plots of k_{obs} *versus* [catalyst] of ligands **4b**, **5b** and **6b** for the cleavage of HPNPP are shown in Fig. 4, and the fitting results of the plots are listed in Table 2. The kinetic data clearly indicates that *N*-methylation of the [12]aneN$_3$ units reduced the catalytic activity, which can be attributed to the steric effects. For ligand **4b**, both the dinuclear zinc(II) and copper(II) complexes show linear dependence on the catalyst concentrations (the plot for Cu_2-**4b** shown as Figure 11S). The plots of Zn_2-**5b** and Zn_2-**6b**, which respectively contain two methyl and four methyl groups on the [12]aneN$_3$ units, show saturation behavior, the data were analyzed by standard Michaelis–Menten kinetics (eqn (3)).

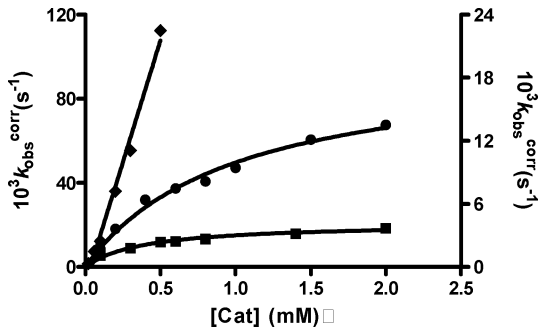

Fig. 4 Plots of k_{obs} *vs.* Zn_2-**L** (L = **4b**, **5b** ●, **6b** ■) for the cleavage of HPNPP (4.0×10^{-5} M) at [$^-$OCH$_3$]/[Zn(II)] = 0.5, ^s_spH = 10.0 ± 0.1 for Zn_2-**4b** (left axis), ^s_spH = 9.9± 0.1 for Zn_2-**5b** (right axis) and ^s_spH = 9.8 ± 0.1 for Zn_2-**6b** (right axis), 25.0 ± 0.1 °C.

For the dinuclear zinc(II) complexes of ligands **4d** and **4g**, which contain 5-substituted nitro-, and carboxyl- moieties, their catalytic activity (Figure 6S) is reduced when compared to that of Zn_2-**4b**. The same is true for the dinuclear copper(II) complex Cu_2-**4d**, which also shows saturation kinetics with k^{max} of (1.22 ± 0.25) × 10^{-2} s^{-1} (see Figure 10S).

The Zn_2-**4b** complex shows the highest catalytic activity and synergistic effect among the zinc(II) complexes in this series. The second-order rate constant is (231 ± 12) M^{-1} s^{-1}, which is approximately 61-fold that of Zn-**1**, and 13-fold higher than that of Zn-[12]aneN$_3$. With a second-order rate constant of (209 ± 2) M^{-1} s^{-1}, Cu_2-**4b** also showed the highest catalytic activity and synergistic effect (10-fold higher than that of Cu-**1**) among the copper(II) complexes in this work. At 1.0 mM of Zn_2-**4b** and Cu_2-**4b**, the cleavage of HPNPP was accelerated by 2.6×10^8-fold and 3.0×10^9-fold, respectively, when compared to that of the background reactions. *N*-Methylation of the [12]aneN$_3$ units in Zn_2-**5b** and Zn_2-**6b** reduced the synergistic effects to be only 5 and 3-fold, respectively, when compared to that of Zn-**1**.

c) Mechanism of the catalytic cleavage of HPNPP. Kinetic data for the mono-nuclear complexes M-**1** and M-**2** indicated a bimolecular process in the studied concentration range. For ligand **1**, the bimolecular process was dependent on both the neutral (CH$_3$OH):M-**1** and basic (CH$_3$O-):M-**1** forms with the former acting to bind the HPNPP and the latter delivering a M(II)-bound methoxide that acts as a base to deprotonate the 2-hydroxypropyl group, similar to that of Zn-[12]aneN$_3$.[29] Both species worked synergistically, resulting in the upward kinetic plot of k_{obs} *versus* [M-**1**]. The activity of Zn-**1** (k_2 = 3.8 M^{-1} s^{-1}) is lower than that of Zn-[12]aneN$_3$ (k_2 = 18.9 M^{-1} s^{-1}),[29] which can be attributed to the steric effect of the benzyl moiety. Less of a decrease on the catalytic activity for Cu-**1** may be attributed to the strong coordination constants between [12]aneN$_3$ and the copper(II) ion. For ligand **2**, the bimolecular process afforded the bowed kinetic curve due to the formation of an inactive dimer in which the coordination of the triazole moiety to the metal ion reduced the free coordination sites for the activation of the phosphates substrate or the nucleophile. Compared with the zinc(II) complex, the catalytic activity of Cu-**2** decreased greatly because of the strong coordination of the triazole moiety to the copper(II) ion.

For the cleavage of HPNPP by a dinuclear Zn(II) complex of PP-Di-[12]aneN$_3$ ligand, Brown *et al.* proposed the process involving at least two binding events, followed by one or more chemical steps that released the observed *p*-nitrophenol product. The binding steps were suggested to consist of phosphate diester association with one metal ion followed by a rearrangement where it became doubly activated *via* binding to the second metal ion. The chemical step was proposed to involve internal deprotonation of the 2-hydroxyl group followed by cyclization with expulsion of the phenoxy leaving group. The catalytic process of the dinuclear metal complexes of ligands **3(b,d,e)**–**6** should be consistent with the same mechanism (see Scheme 6). However, depending on the structure of the ligands and the nature of the metal ions, the synergistic effects between two the [12]aneN$_3$ units and the rate-limiting steps should differ.

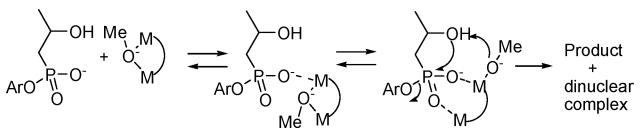

Scheme 6 Pathway for the cleavage of HPNPP promoted by dinuclear metal complexes.

From the kinetic data listed in Table 2, most of the dinuclear metal complexes studied show synergistic effects but they varied from 3- to 700-fold enhancements. After correcting for the inhibition by triflate, the plots of k_{obs} *versus* the concentration of Zn_2-**3b**, Zn_2-**3d**, Zn_2-**4b**, and Cu_2-**4b** are linear, this may indicate that the reactions are limited by a prior binding process and that the actual chemical step of HPNPP cyclization is even faster. In terms of the k_2 values listed in Table 2, the activities of Zn_2-**3b**, Zn_2-**3d**, Zn_2-**4b**, and Cu_2-**4b** are 7.9×10^5, 3.9×10^4, 9.0×10^4, and 8.1×10^4-fold higher than that of methoxide. When compared to that of Zn_2-**PP-Di-[12]aneN$_3$**, the activities of the above dinuclear complexes are 2–3 orders lower, which can be

attributed to the weaker substrate binding ability of the catalysts caused by some of the following factors: the rigidity of the benzene backbone, the large distance between the two 12[ane]N_3 units, and the coordination of triazole moieties to metal(II) ions.

When the substrate binding ability becomes even weaker due to the above aspects, the limiting step of the catalytic reaction will move to the chemical step and the saturation kinetics will appear. This should be the case for the reactions catalyzed by the dinuclear metal complexes Zn_2-**3e**, Zn_2-**4d**, Zn_2-**4g**, Zn_2-**5b**, and Zn_2-**6b** listed in Table 2. It can be seen that steric effects from 2/5-positioned substituents (**3e**, **4d**, **4g**), or *N*-methylation of [12]aneN_3 units (**5b**, **6b**) all significantly impaired the catalytic efficiency and resulted in the Michaelis–Menten saturation kinetics for the cleavage of HPNPP. The rate-limiting step can be assigned to the chemical step of cyclization.

Conclusions

In the present study, we have designed and synthesized a series of mono- and di-[12]aneN_3 ligands **1–6** through nitrogen alkylation and copper(I)-mediated alkyne-azide click reactions. All of the new ligands have been fully characterized by ^{1}H-NMR, ^{13}C-NMR, IR, and MS.

The catalytic activities of their zinc(II) and copper(II) complexes on the cleavage of RNA model phosphate HPNPP have been evaluated, which varied greatly with metal ions and the structures of the ligands. The incorporation of the triazole moieties in the ligands reduced the catalytic activities due to their coordination with metal ions, especially for copper(II) complexes. It was also found that the inhibition of counter ion triflate on the activity is much strong for the dinuclear metal complexes containing triazole moieties. For the ligands lacking triazole moieties, their metal complexes showed good intermolecular (for mononuclear complexes) or intramolecular (for dinuclear complexes) synergistic effects between two metal ions. Specifically, dinuclear complexes Zn_2-**3b**, Zn_2-**3d**, Zn_2-**4b** and Cu_2-**4b** exhibit second-order rate constants of 2.03×10^3, 99.6, 231, and 209 M^{-1} s^{-1}, respectively, which are 7.9×10^5, 3.9×10^4, 9.0×10^4, and 8.1×10^4-fold larger than that of methoxide ($k_2^{MeO-} = 2.56 \times 10^{-3}$ M^{-1} s^{-1}),[31] they afforded the synergistic effects of 700, 42, 61, and 10-fold when compared with the corresponding mononuclear complexes. Relative to the background reactions, the cleavage of HPNPP catalyzed by 1.0 mM of Zn_2-**4b**, and Cu_2-**4b** can be accelerated by 2.6×10^8 and 3.0×10^9-fold, respectively.

The above work clearly demonstrates that substituents on the coordinating backbone, linkers between two [12]aneN_3 units, and the *N*-methylation on [12]aneN_3 units all play important roles in the catalytic activity. The *meta*-positioned di-[12]aneN_3 system showed good activity and evident synergistic effects. The presence of 5/2-positioned substituents on the aryl group and the methyl groups on [12]aneN_3 units resulted in poor activities due to the steric effects.

It should be noted that there is difference in the cleavage mechanism between HPNPP and RNA. For HPNPP, the formation of phosphane is generally the rate-limiting step due to the presence of a good leaving group (4-nitrophenolate). With RNA, the breakdown of the phosphane intermediate is rate-limiting due to the poor leaving property of the alkoxyl group. More [12]aneN_3-derived compounds and their metal complexes are being constructed in our laboratory, their applications on the catalytic cleavage of the phosphate diester linkage in RNA and DNA are currently under investigation.

Experimental

1. Physical measurements

^{1}H- and ^{13}C-NMR spectra were recorded on a Bruker Avance 400 MHz spectrometer and chemical shifts in ppm are reported relative to internal tetramethylsilane (TMS) or residual solvent peaks. IR spectra were recorded on a Nicolet 380 spectrometer in the range of 4000–400 cm^{-1}, samples were prepared as KBr pellets. ESI-MS and HRMS spectra were recorded on Quattro Mocro and Bruker Daltonics Bio TOF mass spectrometer, respectively. UV-visible spectra were obtained on a Varian Cary-300 UV-visible spectrophotometer. Elemental analyses were obtained on an Elementar Vario EL analyzer.

2. Chemicals

Methanol (water < 50 ppm) was purchased from Acros Organics and used as supplied. Sodium methoxide, propargyl bromide, $Cu(CF_3SO_3)_2$, and $Zn(CF_3SO_3)_2$ were purchased from Alfa Aesar and used without further purification. The sodium salt of 2-hydroxylpropyl-*p*-nitrophenyl phosphate (HPNPP) was prepared according to the literature procedure.[31] Compound **1**,[34] **7**,[35] **9**,[36] **10a–f**,[37–44] and **13**[26] were synthesized according to the literature procedures and characterized by ^{1}H-NMR. Other chemicals and reagents were obtained commercially and used without further purification.

3. Synthesis

(1) Preparation of compound 8. Boc_2-[12]aneN_3 **7** (1.86 g, 5 mmol), propargyl bromide (0.59 g, 5 mmol), and triethylamine (0.71 g, 7 mmol) were dissolved in 50 mL of dry THF and stirred under N_2. The reaction mixture was heated to reflux under N_2 for 72 h, and then was evaporated under reduced pressure to afford the crude product. The pure product was separated on a silica gel column (petroleum ether/acetone = 2 : 1, R_f 0.7) to give a white solid. Yield: 1.88 g, 92%. ^{1}H NMR (400 MHz, $CDCl_3$, ppm): δ 3.38 (s, 2H), 3.33–3.25 (m, 8H), 2.54–2.51 (t, J = 12.0 Hz, 4H), 2.16 (s, 1H), 1.88–1.77 (m, 6H), 1.45 (s, 18H). ^{13}C NMR (101 MHz, $CDCl_3$, ppm): δ 156.47, 79.41, 78.06, 73.13, 50.11, 46.20, 44.36, 39.95, 28.69, 26.98, 26.07. HR-MS (*m*/*z*) found (calcd) for $C_{22}H_{39}N_3NaO_4$ $(M + Na)^+$: 432.2860 (432.2838).

(2) Preparation of compound 11(a, b, c, d, e). General method: Compound **10** (1.0 mmol) and NaN_3 (0.33 g, 3.0 mmol) were stirred in THF/H_2O (v/v = 5 : 1) for 2 h. The mixture was extracted with ethyl acetate; the organic layers were combined, washed three times with brine, and subsequently dried with anhydrous Na_2SO_4. After the solvent was removed under reduced pressure, the obtained pale yellow liquid was further dried under vacuum.

11a):[21] Yield: 0.17 g, 91%. ^{1}H NMR (400 MHz, $CDCl_3$, ppm): δ 7.39 (m, 4H), 4.44 (s, 4H).^{13}C NMR (101 MHz, $CDCl_3$, ppm): δ 133.9, 130.2, 129.0, 52.3. ESI-MS (*m*/*z*) found (calcd) for $C_8H_8N_6$ (M): $[M + 1]^+$, 190.17 (189.20).

11b):[21] Yield: 0.165 g, 88%. ^{1}H NMR (400 MHz, $CDCl_3$, ppm): δ, 7.42–7.38 (t, J = 8.0 Hz, 1H), 7.30 (s, 1H), 7.28 (s, 2H), 4.35 (s, 4H).^{13}C NMR (101 MHz, $CDCl_3$, ppm): δ 134.9, 128.1, 126.8, 126.6, 52.2. ESI-MS (m/z) found (calcd) for $C_8H_8N_6$ (M): $[M + 1]^+$, 190.29 (189.20).

11c):[21] Yield: 0.18 g, 96%. ^{1}H NMR (400 MHz, $CDCl_3$, ppm): δ 7.35 (s, 4H), 4.36 (s, 4H). ^{13}C NMR (101 MHz, $CDCl_3$, ppm) δ 133.9, 130.2, 129.0, 52.3. ESI-MS (m/z) found (calcd) for $C_8H_8N_6$ (M): $[M + 1]^+$, 190.11 (189.20).

11d): Yield: 0.22 g, 96%. ^{1}H NMR (400 MHz, $CDCl_3$, ppm): δ 8.16 (s, 2H), 7.65 (s, 1H), 4.55 (s, 4H). ^{13}C NMR (101 MHz, $CDCl_3$, ppm): δ 148.6, 138.5, 132.9, 122.3, 53.5. ESI-MS (m/z) found (calcd) for $C_8H_7N_7O_2$ (M): $[M + 1]^+$, 234.10 (234.19).

11e): Yield: 0.29 g, 98%. ^{1}H NMR (400 MHz, $CDCl_3$, ppm): δ 6.95 (s, 2H), 4.50 (s, 4H), 3.84 (s, 3H). ^{13}C NMR (101 MHz, $CDCl_3$, ppm): δ 156.7, 134.7, 112.8, 112.2, 53.3, 52.6. ESI-MS (m/z) found (calcd) for $C_8H_9BrN_6O$ (M): $[M + 1]^+$, 298.14 (298.12).

(3) Preparation of compound 12(b, d, f). General method: compound **10** (1 mmol) and tricyclic orthodiamide **13** (0.36 g, 3 mmol) in 60 mL freshly distilled $CHCl_3$ was refluxed for 2 h. After cooling to room temperature, the white precipitates were filtered, washed with ether (2 × 10 mL), and then dried to afford the corresponding compounds.

12b): Yield: 0.57 g, 92%. ^{1}H NMR (400 MHz, D_2O, ppm): δ 7.97 (s, 2H), 7.32 (t, J = 7.4 Hz, 1H), 7.16–7.18 (d, J = 7.4 Hz, 2H), 7.04 (s, 1H), 3.74 (s, 4H), 3.59–3.66 (t, J = 13.0 Hz, 4H), 3.17–3.37 (m, 12H), 2.89–2.93 (d, J = 13.5 Hz, 4H), 2.33–2.40 (t, J = 12.8 Hz, 4H), 2.01–2.12 (m, 8H), 1.20–1.24 (d, J = 14.4 Hz, 4H), ^{13}C NMR (400 MHz, D_2O, ppm): δ 156.42, 135.23, 133.22, 129.99, 128.30, 55.33, 54.34, 53.34, 42.26, 22.46, 19.25. IR (KBr, cm^{-1}): 2943 (m), 2839 (m), 1679 (s), 1503 (w), 1459 (m), 1426 (m), 1371 (m), 1332 (m), 1216 (m), 1116 (m), 1070 (m), 1044 (m), 736 (m), 676 (m), 532 (m), 459 (m), 436 (m). ESI-MS (m/z) found (calcd) for $C_{28}H_{46}Br_2N_6$ (M): $[M - Br]^+$, 545.4(545.3), 547.3(547.3).

12d): Yield: 0.64 g, 96%. ^{1}H NMR (400 MHz, D_2O, ppm): δ 7.92 (s, 2H), 7.89 (s, 2H), 7.32 (s, 1H), 3.75 (s, 4H), 3.57–3.50 (t, J = 28 Hz, 4H), 3.28–3.07 (m, 12H), 2.83–2.80 (d, J = 12 Hz, 4H), 2.30–2.37 (t, J = 26.4 Hz, 4H), 2.06–1.85 (m, 8H), 1.17–1.13 (d, J = 14.6 Hz, 4H). ^{13}C NMR (101 MHz, D_2O, ppm): δ 156.30, 147.80, 139.02, 137.27, 124.24, 55.21, 54.52, 53.05, 42.18, 22.69, 19.15. ESI-MS (m/z) found (calcd) for $C_{28}H_{45}Br_2N_7O_2$ (M): $[M - Br]^+$, 591.33(591.61).

12f): Yield: 0.62 g, 90%. ^{1}H NMR (400 MHz, D_2O, ppm): δ 8.03 (s, 2H), 7.77 (s, 2H), 7.33 (s, 1H), 3.86 (s, 4H), 3.75 (s, 3H), 3.66–3.62 (d, J = 12.3 Hz, 4H), 3.39–3.33 (d, J = 12 Hz, 4H), 3.26–3.18 (m, 8H), 2.94–2.91 (d, J = 12 Hz, 4H), 2.50–2.44 (t, J = 16 Hz, 4H), 2.17–2.10 (m, 4H), 2.00–1.88 (m, 4H), 1.29–1.25 (d, J = 16 Hz, 4H). ^{13}C NMR (101 MHz, D_2O, ppm): δ 168.80, 156.34, 137.77, 137.71, 130.57, 129.63, 55.26, 54.30, 52.92, 47.34, 42.32, 23.19, 19.32. ESI-MS (m/z) found (calcd) for $C_{30}H_{48}Br_2N_6O_2$ (M): $[M - Br]^+$, 604.00(604.64).

(4) Preparation of compound 2 and 3(a, b, c, d, e). General method: the respective azide compound (1.0 mmol for **2**, 0.5 mmol for **3**) and compound **8** (0.41 g, 1 mmol) were added into THF/H_2O (v/v = 2 : 1), $CuSO_4 \cdot 5H_2O$ (0.013 g, 0.05 mmol) and sodium vitamin C (0.019 g, 0.1 mmol) were also added into the solution as catalyst. The mixture was stirred overnight at room temperature, saturated with NaCl, and extracted with ethyl acetate. The organic layers were washed once with brine, dried over Na_2SO_4, and evaporated under reduced pressure. The crude products were purified by flash chromatography on silica gel with CH_2Cl_2/MeOH to yield the Boc-protected compounds. Subsequently, the respective Boc-protected compound was dissolved in CH_3OH (40 mL). Acetyl chloride (15 mL) was added dropwisely into the solution and stirred at room temperature for 2 h. After the solvent was removed under reduced pressure, the resultant white precipitates were collected, washed with ether, and dried under vacuum.

2·4HCl): 0.46 g, Yield: 94%. ^{1}H NMR (400 MHz, D_2O, ppm): δ 7.98 (s, 1H), 7.31–7.23 (m, 5H), 5.51 (s, 2H), 3.97 (s, 2H), 3.21–3.13 (m, 8H), 3.87 (s, 4H), 2.16–2.13 (t, J = 11.2 Hz, 2H), 1.97–1.94 (t, J = 12 Hz, 4H). ^{13}C NMR (101 MHz, D_2O, ppm): δ 134.50, 129.13, 128.84, 128.13, 126.53, 54.09, 48.77, 47.45, 43.08, 41.75, 19.83, 18.93. IR (KBr, cm^{-1}): 3423 (s), 2951 (s), 2754 (s), 2635 (s), 1589 (s), 1456 (s), 1364 (w), 1231 (w), 1127 (w), 1055 (m), 1006 (w), 913 (w), 855 (w), 725 (m). Elemental analysis calcd (%) for $C_{19}H_{34}Cl_4N_6$: C, 46.73; H, 7.02; N, 17.21. Found (%): C, 46.33; H, 7.10; N, 17.12. HR-MS (m/z) found (calcd.) for $C_{19}H_{31}N_6$ (M): $[M + H]^+$, 343.2604 (343.2610).

3a·8HCl): 0.41 g, Yield: 92%. ^{1}H NMR (400 MHz, D_2O, ppm): δ 8.19 (s, 2H), 7.34 (m, 4H), 5.62 (s, 4H), 4.31 (s, 4H), 3.31–3.21 (m, 24H), 2.24–2.14 (m, 12H).^{13}C NMR (101 MHz, D_2O, ppm): δ 137.72, 135.02, 128.77, 127.17, 53.60, 48.77, 47.99, 42.30, 41.17, 19.88, 18.32. IR (KBr, cm^{-1}): 3441 (s), 2951 (s), 2642 (s), 2407 (s), 1590 (s), 1517 (w), 1482 (s), 1458 (s), 1440 (s), 1365 (m), 1213 (s), 1132 (m), 1055 (m), 1005 (s), 917 (m), 855 (w), 794 (w), 746 (m), 522 (m). Elemental analysis calcd (%) for $C_{32}H_{62}Cl_8N_{12}$: C, 42.77; H, 6.95; N, 18.71. Found (%): C, 42.64; H, 7.13; N, 18.61. HR-MS (m/z) found (calcd.) for $C_{32}H_{54}N_{12}$ (M): $[M + H]^+$, 607.4674 (607.4673).

3b·8HCl): 0.42 g, Yield: 93%. ^{1}H NMR (400 MHz, D_2O, ppm): δ 8.17 (s, 2H), 7.43–7.39 (t, J = 16 Hz, 1H), 7.31–7.29 (d, J = 6.4 Hz 3H), 5.62 (s, 4H), 4.28 (s, 4H), 3.33–3.28 (m, 16H), 3.17 (s, 8H), 2.25–2.23 (t, J = 5.6 Hz, 4H), 2.15–2.12 (t, J = 6.0 Hz, 8H). ^{13}C NMR (101 MHz, D_2O, ppm): δ 136.90, 135.37, 129.89, 128.46, 127.63, 53.73, 48.54, 47.55, 42.10, 41.08, 19.97, 18.01. IR (KBr, cm^{-1}): 3422 (s), 2959 (s), 2757 (s), 2641 (s), 1616 (m), 1588 (m), 1479 (m), 1457 (m), 1434 (m), 1364 (w), 1233 (w), 1128 (w), 1057 (m), 1006 (w), 913 (w), 747 (m). Elemental analysis calcd (%) for $C_{32}H_{62}Cl_8N_{12}$: C, 42.77; H, 6.95; N, 18.71. Found (%): C, 42.66; H, 7.21; N, 18.68. HR-MS (m/z) found (calcd.) for $C_{32}H_{54}N_{12}$ (M): $[M + H]^+$, 607.4668 (607.4673).

3c·8HCl): 0.41 g, Yield: 91%. ^{1}H NMR (400 MHz, D_2O, ppm): δ 8.10 (s, 2H), 7.60 (s, 2H), 7.32 (s, 2H), 5.69 (s, 4H), 4.37 (s, 4H), 3.28–3.23 (m, 24H), 2.15 (m, 12H).^{13}C NMR (101 MHz, D_2O, ppm): δ 136.46, 132.50, 130.76, 130.03, 127.61, 51.39, 48.48, 47.28, 41.89, 40.90, 19.94, 17.83. IR (KBr, cm^{-1}): 3442 (s), 2960 (s), 2760 (s), 2635 (s), 2413 (s), 1616 (s), 1483 (s), 1458 (s), 1214 (s), 1053 (m), 1005 (s), 919 (m), 747 (m), 523 (m). Elemental analysis calcd (%) for $C_{32}H_{62}Cl_8N_{12}$: C, 42.77; H, 6.95; N, 18.71. Found (%): C, 42.71; H, 6.99; N, 18.65. HR-MS (m/z) found (calcd.) for $C_{32}H_{54}N_{12}$ (M): $[M + H]^+$, 607.4674 (607.4673).

3d·8HCl): 0.39 g, Yield: 82%. ^{1}H NMR (400 MHz, D_2O, ppm): δ 8.19 (s, 2H), 8.07 (s, 2H), 7.07 (s, 1H), 5.76 (s, 4H), 4.18 (s, 4H), 3.32–3.27 (m, 17H), 3.07 (m, 7H), 2.27–2.24 (t, J = 12 Hz, 4H), 2.11–2.08 (t, J = 12 Hz, 8H). ^{13}C NMR (101 MHz, D_2O, ppm): δ 148.55, 137.37, 133.96, 126.66, 122.97, 122.55, 57.36, 52.80, 49.53,

42.13, 19.88, 19.44, 16.73. IR (KBr, cm^{-1}): 3431 (s), 2956 (m), 2928 (m), 2759 (s), 2105 (m), 1619 (m), 1590 (m), 1537 (s), 1456 (s), 1351 (s), 1232 (w), 1122 (w), 1055 (m), 1007 (w), 916 (w), 787 (w), 738 (m). Elemental analysis calcd (%) for $C_{32}H_{61}Cl_8N_{12}O_2$: C, 40.73; H, 6.52; N, 19.30. Found (%): C, 40.68; H, 6.40; N, 19.10. HR-MS (*m/z*) found (calcd.) for $C_{32}H_{53}N_{12}O_2$ (M): $[M + H]^+$, 652.4532 (652.4523).

3e·8HCl): 0.43 g, Yield: 85%. ^{1}H NMR (400 MHz, D_2O, ppm): δ 8.19 (s, 2H), 6.98 (s, 2H), 5.70 (s, 4H), 4.31 (s, 4H), 3.77 (s, 3H), 3.34–3.29 (m, 17H), 3.21 (s, 7H), 2.26–2.23 (t, J = 12 Hz, 4H), 2.16–2.13 (t, J = 12 Hz, 8H). ^{13}C NMR (101 MHz, D_2O, ppm): δ 158.82, 138.27, 135.76, 127.37, 117.61, 115.89, 55.77, 54.64, 48.61, 47.67, 42.91, 41.63, 19.93, 18.80. IR (KBr, cm^{-1}): 3407 (m), 3224 (m), 3084 (w), 2910 (w), 2881 (w), 1531 (s), 1465 (m), 1419 (s), 1392 (s), 1342 (s), 1197 (m), 1150 (m), 1096 (m), 1063 (m), 1038 (m), 928 (w), 868 (m), 784 (m), 746 (m), 695 (w), 651 (m). Elemental analysis calcd (%) for $C_{33}H_{63}BrCl_8N_{12}O$: C, 39.34; H, 6.30; N, 16.68. Found (%): C, 39.45; H, 6.46; N, 16.28. HR-MS (*m/z*) found (calcd.) for $C_{33}H_{55}BrN_{12}O$ (M): $[M + H]^+$, 715.3914 (715.3883).

(5) Preparation of compound 4(b, d, g). General method for preparing compounds **4**(**b**, **d**): compounds **12**(**b** or **d**) (0.5 mmol) in 20 mL of 3 M HCl was refluxed for 12 h, and then neutralized with NaOH solution of water (3.0 M) until alkaline (pH ≥ 12). The mixture was then extracted with CH_2Cl_2 (30 mL × 4). After the combined organic layers were dried over anhydrous Na_2SO_4, the solvent was removed by rotary evaporation under reduced pressure to afford the free ligand as a pale yellow viscous oil.

Method for compound **4g**: compound **12g** (0.5 mmol) in 20 mL of 3 M HCl was refluxed for 12 h, and then the solvent was removed in rotary under reduced pressure to afford the ligand as a white solid, which was washed twice with ethanol.

4b): Yield: 0.16 g, 71%. ^{1}H NMR (400 MHz, $CDCl_3$, ppm): δ 7.28–7.30 (m, 3H), 7.23 (s, 1H), 3.50 (s, 4H), 2.85 (m, 8H), 2.71 (m, 8H), 2.53 (m, 8H), 1.69–1.74 (m, 12H).^{13}C NMR (101 MHz, $CDCl_3$, ppm): 138.93, 129.85, 127.94, 127.46, 57.35, 52.51, 49.48, 46.85, 26.45, 26.02. IR (KBr, cm^{-1}): 3317 (m), 2928 (s), 2801 (s), 1667 (s), 1452 (s), 1431 (s), 1398 (m), 1374 (m), 1265 (m), 1246 (m), 1204 (m), 1176 (m), 1148 (m), 1095 (m), 1068 (m), 800 (w), 734(m), 700 (w). Elemental analysis calcd (%) for $C_{26}H_{48}N_6$: C, 70.22; H, 10.88; N, 18.90. Found (%): C, 69.98; H, 10.97; N, 18.65. HR-MS (*m/z*) found (calcd.) for $C_{26}H_{48}N_6$ (M): $[M + H]^+$, 445.3952 (445.3941).

4d): Yield: 0.21 g, 84%. ^{1}H NMR (400 MHz, $CDCl_3$, ppm): δ 8.25 (s, 2H), 7.61 (s, 1H), 3.57 (s, 4H), 2.89–2.86 (t, J = 10.0 Hz, 8H), 2.70–2.67 (t, J = 10.2 Hz, 8H), 2.56–2.53 (t, J = 10.9 Hz, 8H), 1.73–1.68 (m, 12H). ^{13}C NMR (101 MHz, $CDCl_3$, ppm): δ 148.64, 141.98, 135.19, 122.10, 56.95, 52.84, 50.13, 47.17, 26.58, 26.19. IR (KBr, cm^{-1}): 3421 (s), 2951 (s), 2753 (br, s), 1653 (s), 1588 (s), 1537 (s), 1459 (s), 1353 (s), 1177 (w), 1108 (m), 1069 (m), 1006 (m), 887 (m), 784 (m), 746 (s), 694 (m), 556 (br, m). Elemental analysis calcd (%) for $C_{26}H_{47}N_7O_2$: C, 63.77; H, 9.67; N, 20.02. Found (%): C, 63.57; H, 9.86; N, 19.69. HR-MS (*m/z*) found (calcd.) for $C_{26}H_{48}N_7O_2$ (M): $[M + H]^+$, 490.3884 (490.3869).

4g·5HCl): 0.31 g, Yield: 91%. ^{1}H NMR (400 MHz, D_2O, ppm): δ 8.21 (s, 2H), 7.89 (s, 1H), 4.42 (s, 4H), 3.34–3.32 (m, 24H), 2.25–2.178 (m, 12H). ^{13}C NMR (101 MHz, D_2O, ppm): δ 167.26, 137.96, 133.07, 132.11, 131.54, 62.90, 57.13, 47.51, 44.63, 42.42, 41.25, 40.98, 20.26, 19.05, 18.17, 13.47. IR (KBr, cm^{-1}): 3420 (s), 2960 (s), 2758 (br, s), 1716 (s), 1593 (s), 1458 (s), 1369 (m), 1308 (s), 1227 (s), 1145 (m), 1085 (m), 1071 (m), 1023 (m), 884 (w), 818 (w), 746 (w), 702 (w), 567 (m), 513 (m). Elemental analysis calcd (%) for $C_{27}H_{53}Cl_5N_6O_2$: C, 48.33; H, 7.96; N, 12.52. Found (%): C, 48.17; H, 8.12; N, 12.31. HR-MS (*m/z*): found (calcd.) for $C_{27}H_{49}N_6O_2$ (M): [M + H] 489.3923 (489.3917).

(6) Preparation of compound 5b. Under an argon atmosphere, a solution of **12b** (1.0 g, 1.6 mmol) and $NaBH_4$ (0.59 g, 10 eq) in 50 mL of ethanol was stirred in an ice bath overnight. The reaction mixture was quenched with 6 M HCl, and then neutralized to alkaline (pH ≥ 12) with 50% aqueous NaOH. The mixture was extracted with CH_2Cl_2 (30 mL × 4), and the organic layers were combined together, dried over anhydrous Na_2SO_4. The solvent was then removed *in vacuo* to afford the free ligand as a pale yellow viscous oil. Yield: 0.49 g, 65%. ^{1}H NMR (400 MHz, $CDCl_3$, ppm): δ 7.17–7.20 (m, 4H), 3.38 (s, 4H), 2.70 (m, 4H), 2.55 (m, 4H), 2.43–2.45 (m, 8H), 2.34–2.36 (m, 8H), 2.08 (s, 6H), 1.58–1.61 (m, 12H). ^{13}C NMR(101 MHz, $CDCl_3$, ppm): δ 139.43, 129.63, 128.32, 127.30, 58.31, 57.78, 54.23, 54.07, 50.09, 49.26, 48.39, 40.87, 24.61, 24.21, 18.44. IR (KBr, cm^{-1}): 3321 (m), 2928 (s), 2801 (s), 1712 (s), 1668 (s), 1452 (s), 1431 (s), 1398 (s), 1363 (s), 1221 (m), 1204 (m), 1176 (m), 1148 (m), 1068 (m), 791 (w), 741 (m), 700 (w), 530 (w). Elemental analysis calcd (%) for $C_{28}H_{52}N_6$: C, 71.14; H, 11.09; N, 17.78. Found (%): C, 71.08; H, 10.93; N, 17.62. HR-MS (*m/z*) found (calcd.) for $C_{28}H_{52}N_6$ (M): $[M + 1]^+$, 473.4348 (473.4332).

(7) Preparation of compound 6b. Under an argon atmosphere, a mixture of **12b** (1.0 g, 1.6 mmol), formic acid (10 mL), and formaldehyde solution (10 mL, 37–40%) was refluxed overnight. After the removal of solvent *in vacuo*, the residue was quenched with 6 M HCl, and then neutralized to alkaline (pH ≥ 12) with 50% aqueous NaOH. The solution was extracted with CH_2Cl_2 (30 mL × 4), the organic layers were combined, dried over anhydrous Na_2SO_4, and the solvent was then removed under vacuum to obtain the free ligand as pale yellow viscous oil. Yield: 0.48 g, 60%. ^{1}H NMR (400 MHz, $CDCl_3$, ppm): δ 7.16–7.25 (m, 4H), 3.46 (s, 4H), 2.42–2.47 (m, 24H), 2.20 (s, 12H), 1.59–1.61 (m, 12H). ^{13}C NMR (101 MHz, $CDCl_3$, ppm): δ 139.95, 129.52, 127.79, 127.26, 62.37, 59.13, 57.96, 55.83, 52.25, 49.27, 45.49, 42.99, 42.23, 25.61, 25.27, 22.08. FT-IR (KBr, cm^{-1}): 2934 (s), 2926 (s), 2834 (s), 2788 (s), 1677 (m), 1607 (w), 1589 (w), 1458 (s), 1366 (m), 1344 (m), 1241 (m), 1120 (m), 1102 (m), 1081 (m), 1060 (m), 963 (m), 861 (w), 803 (w), 741 (m), 698 (w), 568 (w). Elemental analysis calcd (%) for $C_{30}H_{56}N_6$: C, 71.95; H, 11.27; N, 16.78. Found (%): C, 71.75; H, 11.64; N, 16.42. HR-MS (*m/z*) found (calcd.) for $C_{30}H_{56}N_6$ (M): $[M + 1]^+$, 501.4651 (501.4645).

4. General methods for kinetic measurements

The $CH_3OH_2^+$ concentrations were determined using a combination glass electrode (Mettler Toledo FE20) calibrated with Fisher Certified standard aqueous buffers (pH 4.00, 7.00 and 10.00) as described in the literature.[45] The ^s_spH values in methanol were determined by subtracting a correction constant of –2.24 from the readings obtained from the electrode, while the autoprotolysis constant was taken to be $10^{-16.77}$ M^2. The values for the kinetic experiments were simply measured from the solution of the complexes after reactions.

The rates of catalyzed cleavage of HPNPP (0.04 mM) were monitored spectrophotometrically using a UV-vis spectrophotometer thermostatted at 25.0 ± 0.1 °C. Reaction rates were determined from the rate of appearance of *p*-nitrophenol at 322 nm. All kinetic experiments were performed with catalyst formed *in situ* through the sequential addition of stock solutions (typically 20 mM) of sodium methoxide, ligand and $Zn(OTf)_2$ or $Cu(OTf)_2$ to anhydrous methanol such that $[^-OCH_3]$: ligand : $[Zn(OTf)_2] = 1:2:2$ for mono-12[ane]N_3 ligands **1** and **2** and $[^-OCH_3]$: ligand : $[Zn(OTf)_2] = 1:1:2$ for di-12[ane]N_3 ligands **3–6** to give a total volume of 2.5 mL in the quartz cuvettes. Formulation of the catalysts in this way yielded self-buffered solutions with ${}^{s}_{s}\mathrm{pH}$ values in the desired range. The reported values of pseudo-first order rate constants (k_{obs}) for the production of *p*-nitrophenol are the averages of duplicate runs.

Acknowledgements

The authors gratefully acknowledge the financial assistance from the Fundamental Research Funds for the Central Universities (2009SC-1), Beijing Municipal Commission of Education; Specialized Research Fund for the Doctoral Program of Higher Education (273911), Program for New Century Excellent Talents at Universities (15770703), the Ministry of Education of China; and the Nature Science Foundation of China (202028). The authors also thank Prof. R. S. Brown, Prof. H. K. Fun, Prof. B. Coppola, and Dr Rui-Bing Wang for their helpful discussions.

Notes and references

1 J. R. Morrow, T. L. Amyes and J. P. Richard, *Acc. Chem. Res.*, 2008, **41**, 539.
2 R. S. Brown and A. A. Neverov, *Adv. Phys. Org. Chem.*, 2008, **42**, 271.
3 J. Weston, *Chem. Rev.*, 2005, **105**, 2151.
4 R. Wolfenden and M. J. Snider, *Acc. Chem. Res.*, 2001, **34**, 938.
5 H. Loennberg, *Org. Biomol. Chem.*, 2011, **9**, 1687.
6 J. J. Zhang, Y. Shao, L. Wei, Y. Li, X. Sheng, F. Liu and G. Y. Lu, *Sci. China, Ser. B: Chem.*, 2009, **52**, 402.
7 J. F. Davies, II, Z. Hostomska, Z. Hostomsky, S. R. Jordan and D. A. Matthews, *Science*, 1991, **252**, 88.
8 A. Lahm, A. Volbeda and D. Suck, *J. Mol. Biol.*, 1990, **215**, 207.
9 J. A. Cowan, *Chem. Rev.*, 1998, **98**, 1067.
10 C. Liu and L. Wang, *Dalton Trans.*, 2009, 227.
11 F. Mancin and P. Tecilla, *New J. Chem.*, 2007, **31**, 800.
12 D. E. Wilcox, *Chem. Rev.*, 1996, **96**, 2435.
13 O. Iranzo, A. Y. Kovalevsky, J. R. Morrow and J. P. Richard, *J. Am. Chem. Soc.*, 2003, **125**, 1988.
14 Z.-L. Lu, C. T. Liu, A. A. Neverov and R. S. Brown, *J. Am. Chem. Soc.*, 2007, **129**, 11642.
15 C. T. Liu, A. A. Neverov and R. S. Brown, *J. Am. Chem. Soc.*, 2008, **130**, 13870.
16 Q. Wang, E. Leino, A. Jancso, I. Szilagyi, T. Gajda, E. Hietamaki and H. Lonnberg, *ChemBioChem*, 2008, **9**, 1739.
17 K. Li, J. Zhang, J.-J. Zhang, Z.-W. Zhang, Z.-J. Zhuang, D. Xiao, H.-H. Lin and X.-Q. Yu, *Appl. Organomet. Chem.*, 2008, **22**, 243.
18 Q.-X. Xiang, J. Zhang, P.-Y. Liu, C.-Q. Xia, Z.-Y. Zhou, R.-G. Xie and X.-Q. Yu, *J. Inorg. Biochem.*, 2005, **99**, 1661.
19 R. S. Brown, Z.-L. Lu, C. T. Liu, W. Y. Tsang, D. R. Edwards and A. A. Neverov, *J. Phys. Org. Chem.*, 2010, **23**, 1.
20 F. Amblard, J. H. Cho and R. F. Schinazi, *Chem. Rev.*, 2009, **109**, 4207.
21 P. Ramirez-Lopez, M. C. de la Torre, H. E. Montenegro, M. Asenjo and M. A. Sierra, *Org. Lett.*, 2008, **10**, 3555.
22 J. Zan, H. Yan, Z.-F. Guo and Z.-L. Lu, *Inorg. Chem. Commun.*, 2010, **13**, 1054.
23 Q. Wang and H. Lonnberg, *J. Am. Chem. Soc.*, 2006, **128**, 10716.
24 P. Hubsch-Weber and M. T. Youinou, *Tetrahedron Lett.*, 1997, **38**, 1911.
25 Y.-W. Ren, H. Guo, C. Wang, J.-J. Liu, H. Jiao, J. Li and F.-X. Zhang, *Transition Met. Chem.*, 2006, **31**, 611.
26 R. W. Alder, R. W. Mowlam, D. J. Vachon and G. R. Weisman, *J. Chem. Soc., Chem. Commun.*, 1992, 507.
27 Z.-L. Lu, C.-Y. Duan, Y.-P. Tian, X.-Z. You and X.-Y. Huang, *Inorg. Chem.*, 1996, **35**, 2253.
28 A. W. Addison, T. N. Rao, J. Reedijk, J. Van Rijn and G. C. Verschoor, *J. Chem. Soc., Dalton Trans.*, 1984, 1349.
29 A. A. Neverov, Z.-L. Lu, C. I. Maxwell, M. F. Mohamed, C. J. White, J. S. W. Tsang and R. S. Brown, *J. Am. Chem. Soc.*, 2006, **128**, 16398.
30 A. A. Neverov and R. S. Brown, *Org. Biomol. Chem.*, 2004, **2**, 2245.
31 J. S. W. Tsang, A. A. Neverov and R. S. Brown, *J. Am. Chem. Soc.*, 2003, **125**, 1559.
32 S. E. Bunn, C. T. Liu, Z.-L. Lu, A. A. Neverov and R. S. Brown, *J. Am. Chem. Soc.*, 2007, **129**, 16238.
33 A. Y. Lebedev, J. P. Holland and J. S. Lewis, *Chem. Commun.*, 2010, **46**, 1706.
34 P. Brunet and J. D. Wuest, *J. Org. Chem.*, 1996, **61**, 1847.
35 X.-H. Bu, S.-L. Lu, R.-H. Zhang, D.-Z. Liao, S. Aoki, T. Clifford and E. Kimura, *Inorg. Chim. Acta*, 2000, **298**, 50.
36 K. Asano and S. Matsubara, *Org. Lett.*, 2010, **12**, 4988.
37 G. P. Miller and J. Mack, *Org. Lett.*, 2000, **2**, 3979.
38 J. C. Lee and E. Y. Hwang, *Synth. Commun.*, 2004, **34**, 2959.
39 C. B. Zhang, Y. Li, W. K. Liu, H. Q. Zhang, H. Yang, Q. S. Li and G. Z. Xing, *Chin. Chem. Lett.*, 2009, **20**, 1423.
40 M. P. Placidi, A. J. L. Villaraza, L. S. Natrajan, D. Sykes, A. M. Kenwright and S. Faulkner, *J. Am. Chem. Soc.*, 2009, **131**, 9916.
41 H. Y. Kuchelmeister and C. Schmuck, *Eur. J. Org. Chem.*, 2009, 4480.
42 G.-J. M. Gruter, O. S. Akkerman and F. Bickelhaupt, *J. Org. Chem.*, 1994, **59**, 4473.
43 K. Krogh-Jespersen, M. Czerw, K. Zhu, B. Singh, M. Kanzelberger, N. Darji, P. D. Achord, K. B. Renkema and A. S. Goldman, *J. Am. Chem. Soc.*, 2002, **124**, 10797.
44 R. Young and C. K. Chang, *J. Am. Chem. Soc.*, 1985, **107**, 898.
45 For the designation of pH in non-aqueous solvents we use the forms recommended by the IUPAC, *Compendium of Analytical Nomenclature. Definitive Rules 1997* 3rd ed., Blackwell, Oxford, U. K., 1998. If one calibrates the measuring electrode with aqueous buffers and then measures the pH of an aqueous buffer solution, the term ${}^{w}_{w}\mathrm{pH}$ is used; if the electrode is calibrated in water and the 'pH' of the neat buffered methanol solution then measured, the term ${}^{s}_{s}\mathrm{pH}$ is used; and if the electrode is calibrated in the same solvent and the 'pH' reading is made, then the term ${}^{s}_{w}\mathrm{pH}$ is used. Since the autoprotolysis constant of methanol is $10^{-16.77}$, neutral ${}^{s}_{s}\mathrm{pH}$ is 8.4.

